its trisulfate salt and has been converted to its hexahydrochloride by using an anion-exchange resin. Compounds **16** and **17** are available from Strem Chemicals, Inc., and were converted to their hydrochloride salts. The sodium salts of ATP and ADP and the lithium-potassium salt of acetyl phosphate were obtained from Boehringer Mannheim. All other chemicals used were high-purity commercial products.

Methods. ^{31}P NMR spectra were recorded at 81 MHz on a Bruker SY 200 or at 121.42 MHz on a Varian XL300; chemical shifts in ppm are relative (+, downfield) to an external reference of 85% H_3PO_4. Probe temperature was regulated by a variable-temperature accessory. The use of low decoupler power for heteronuclear decoupling at the reported concentrations of reagents and salts in 5-mm NMR tubes did not result in apparent temperature variations. This contrasts with previous studies wherein, using a 2-mL sample in a 10-mm tube, the temperature was not accurately maintained by the variable-temperature control.[11b]

The solution pH was recorded at 22 or 25 °C with a Metrohm 636 titrimeter; adjustments to the desired pH of 1- or 2-mL samples containing the ligand and substrate were made by using ~5 NaOH or HCl. The buffer used in this study was collidine (pK_a 7.32) at pH 7.6.

Kinetic studies were performed by following the time-dependent change in the integrals from the resolved ^{31}P NMR signals of P_α, P_β, and P_γ of ATP and the peaks for inorganic phosphate, pyrophosphate, acetyl phosphate, and phosphoryl derivatives of the macrocycles **1** and **4**. Calibration curves were employed when the integral ratios were not equal because of variaions in the ^{31}P relaxation times. By this method of analysis the calculated standard deviation for the observed rates was 6%.

In a typical experiment, a 1.0- or 2.0-mL solution containing 0.010 or 0.030 M ATP, the polyamine as its hexahydrochloride or hydrobromide salts (0.010, 0.015, or 0.030 M), and, when indicated, added buffer or salts in 10% D_2O/H_2O were placed in the NMR probe in 5- or 10-mm tubes at the temperature indicated. By the use of a kinetic program an adequate number of acquisitions were accumulated for each sequential spectrum over a period of several half-lives.

Acknowledgment. This work was supported by a grant from the National Institute of General Medical Sciences (GM 33922) at the University of Kansas and by the Centre National de la Recherche Scientifique (CNRS) at the University of Louis Pasteur. We also acknowledge the technical assistance of Paulos Yohannes and Paula Martin of the University of Kansas. Compounds **14** and **15** have been prepared by Dr. Bernard Dietrich (University of Louis Pasteur) in the course of other work.[37,38b]

Registry No. 1, 43090-52-4; **2**, 105763-00-6; **4**, 297-11-0; **6**, 58512-71-3; **7**, 56187-15-6; **9**, 862-28-2; **10**, 105763-01-7; ATP, 56-65-5; ADP, 58-64-0; acetyl phosphate lithium potassium salt, 94249-01-1; pyrophosphate, 14000-31-8.

Diabatic Surfaces for Two-Bond Addition Reactions. The Role of Resonance Interaction

Fernando Bernardi,*† Massimo Olivucci,† Joseph J. W. McDouall,‡ and Michael A. Robb*‡

Contribution from the Istituto Chimico G. Ciamician, Università di Bologna, Bologna, Italy, and the Department of Chemistry, Kings College London (KQC), Strand, London WC2R 2LS, England. *Received October 10, 1985*

Abstract: Diabatic surfaces for two-bond cycloaddition reactions are examined in terms of a diabatic surface analysis which includes the computation of the resonance interaction between the reactant-like and product-like diabatic surfaces. A qualitative analysis and rigorous numerical computations are presented for a concerted synchronous mechanism (a two-bond process), a concerted asynchronous mechanism (a concerted one-bond process), and the first step of a two-step mechanism (a nonconcerted one-bond process) for both "allowed" and "forbidden" processes. The results illustrate that the resonance interaction is the dominant factor which controls the mechanistic preference between two-bond and one-bond processes. For a Woodward-Hoffmann forbidden process, the magnitude of the resonance interaction is found to be much smaller for the (forbidden) synchronous process than for the one-bond process; this leads to the expected preference for the one-bond process. For a Woodward-Hoffmann allowed process in the comparison of a concerted two-bond mechanism and the first step of a two-step mechanism, it is found that magnitude of the resonance interaction at the transition structure geometry can lead to a preference for the concerted process.

1. Introduction

In a recent paper, Dewar[1] has examined, qualitatively, the mechanisms of two-bond reactions by using the Evans-Polanyi[2]/Evans-Warhurst[3] diabatic surface model. As a result of this analysis, Dewar was able to derive the rule that *synchronous multibond mechanisms are normally prohibited*. Furthermore, exceptions to this rule were to be expected[1,2] when the transition state for the synchronous multibond mechanism is strongly stabilized by the *resonance interaction* between reactant-like and product-like diabatic surfaces. Dewar[1] has suggested that this situation is most likely to occur for Woodward-Hoffmann *allowed* reactions. Our objective in this paper is to examine this conjecture in some detail for the particular case of two-bond additions. We shall proceed first in a similar fashion to Dewar[1] with qualitative arguments and then present the results obtained with a quantum mechanical implementation of the same model for a few examples.

Recently we have developed[4,5] a method for the quantitative analysis of potential energy surfaces in terms of diabatic surface methods, first proposed by Evans et al.[2,3] This analysis has been applied successfully to our MC-SCF transition structure computations on the 1,2- and 1,3-sigmatropic shift in propene,[6] the cycloaddition of two ethylenes,[7,8] and the 1,3-dipolar cycloaddition

† Università di Bologna.
‡ Kings College London.

(1) Dewar, M. J. S. *J. Am. Chem. Soc.* **1984**, *106*, 209.
(2) Evans, M. G.; Polanyi, J. *Trans. Faraday Soc.* **1938**, *34*, 614.
(3) Evans, M. G.; Warhurst, E. *Trans. Faraday Soc.* **1938**, *34*, 11.
(4) (a) Bernardi, F.; Robb, M. A. *Mol. Phys.* **1983**, *48*, 1345. (b) Bernardi, F.; Demetrakl Paleolog, S. A. H.; McDouall, J. J. W.; Robb, M. A. *J. Molec. Struct. (THEOCHEM)* **1986**, *138*, 23. (c) Bernardi, F.; McDouall, J. J. W.; Robb, M. A. *J. Comput. Chem.*, in press.
(5) Bernardi, F.; Robb, M. A. *J. Am. Chem. Soc.* **1984**, *106*, 54.
(6) Bernardi, F.; Robb, M. A.; Schlegel, H. B.; Tonachini, G. *J. Am. Chem. Soc.* **1984**, *106*, 1198.
(7) Bernardi, F.; Bottoni, A.; Robb, M. A.; Schlegel, H. B.; Tonachini, G. *J. Am. Chem. Soc.* **1985**, *107*, 2260.

0002-7863/87/1509-0544$01.50/0

of acetylene and fulminic acid.[9] In these calculations we were able to correlate the transition structures with diabatic surface intersections. The important feature of the model proposed in ref 4 and 5 is the association of the reactant-like bonding situation or the product-like bonding situation with diabatic surfaces constructed from wave functions built from the molecular orbitals of the isolated fragments. Thus, the diabatic surfaces are based upon a linear combination of Heitler–London, no-bond, and charge-transfer configurations that are familiar from valence-bond approaches (see for example, ref 10).

In our previous diabatic surface work,[4-9] we have used a computational procedure that did not include the calculation of the *resonance interaction* (i.e., interaction matrix element) between the diabatic surfaces. In order to examine the conjecture of Dewar[1] and Evans et al.[2,3] concerning the role of the *resonance interaction* for Woodward–Hoffmann allowed reactions, we have extended our previous computational procedure to enable the calculation of the resonance interaction effect. Further, in previous work we have used the MO of the fragments (an MO-VB approach) to construct the diabatic surfaces. In order to remain close to the VB formalism of Evans,[3] we have used the original Heitler–London (HL-VB) formalism in which the orbitals used in the construction of the diabatics are localized onto atoms.

2. Qualitative Discussion of Two-Bond Reactions within the Evans–Polanyi Diabatic Surface Model

In the diabatic surface model,[2-5] the adiabatic surface of a reaction results from the interaction of two diabatic surfaces: reactant-like and product-like. The transition structure is located near the minimum of the seam of intersection of the two diabatic surfaces. The diabatic surfaces themselves correspond to wave functions built from Heitler–London configurations (involving open-shell spin-coupled fragments), and charge-transfer configurations (electron transfer between fragments). These configurations are constructed from atom-localized MC-SCF orbitals. The adiabatic states are of the complete active-space (CAS) type.

In general, one identifies a bonding situation (reactant-like or product-like) with a Heitler–London configuration. However, in order to describe this *bonding situation* (i.e., diabatic surface), at finite interfragment separation, we must allow for charge transfer. In practical computation, we shall use an effective Hamiltonian (for a comprehensive review see ref 11), in which the diabatic-state energies are obtained as the diagonal matrix elements, the resonance interactions are obtained as the off-diagonal matrix elements, and the adiabatic states are obtained as the eigenvalues. The diabatic states are obtained from the projection of the full CI wave function (built from atom-localized MC-SCF orbitals) onto the subspace of the (product-like and reactant-like) Heitler–London configurations. Thus, the diabatic wave functions are obtained as an orthogonal VB expansion of HL and charge-transfer configurations built from localized orbitals. However (as we shall presently discuss), as a consequence of the projection onto the HL configurations, the adiabatic wave function is obtained as a combination of the projected HL configurations alone. Thus, the diabatic energies corresponding to these projected HL configurations, obtained from the effective Hamiltonian (and the projected HL configurations themselves), must be interpreted as if the HL configurations had been constructed from distorted nonorthogonal AO (as in the Coulson–Fischer[12] calculations on the hydrogen molecule). Charge transfer causes the orthogonal-atom-localized AO to distort, becoming nonorthogonal, and increases the overlap between the orbitals involved in the charge transfer. We now proceed to summarize the main features of this approach.

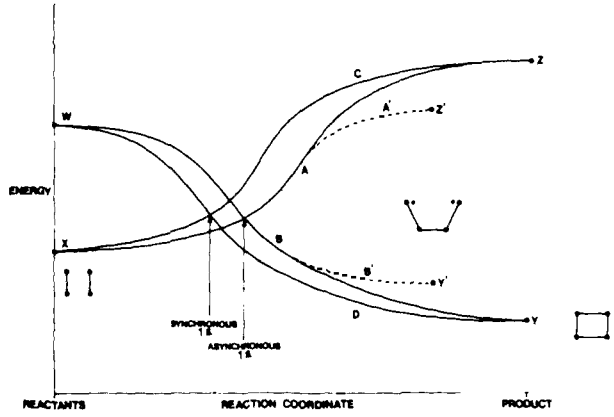

Figure 1. Qualitative diabatic curves for two-bond cycloadditions. (A, A′, B, B′) One-bond process. (C, D) Two-bond process.

Scheme I

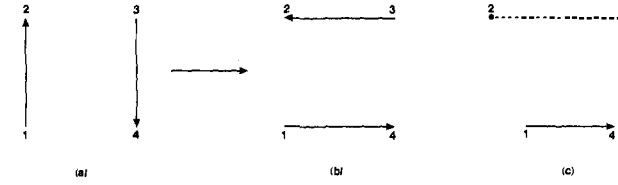

It is appropriate to illustrate the development of the theory with the aid of an example that will describe a two-bond cycloaddition. We assume that the problem can be described by four active orbitals. The reactants have two singlet coupled HL bond eigenfunctions (Ia, 1–2 and 3–4 in Scheme Ia), while in the product (Ib, Scheme Ib) either two new bonds (1–4 and 2–3) are formed or one bond is formed (Ic, 1–4 of Scheme Ic) with a diradical pair (2–3).

We now represent (in a qualitative manner) the energy changes taking place in the reaction of Ia to give either Ib or Ic in terms of the diabatic energies of the bond-breaking process (the energy of the bond eigenfunction Ia) and the bond-forming process (the energy of the bond eigenfunction Ib/Ic) as a function of the reaction coordinate projected onto the shorter of the two new bonds. We intend to justify in some detail that the resultant diabatic curves will have the form given in Figure 1 (in the absence of symmetry).

The curves A/A′ represents the reactant-like diabatic curve for an asynchronous concerted/nonconcerted one-bond reaction (Ia to Ib/Ic), while the curves B/B′ is the analogous product-like diabatic curve. The curves C and D represent the reactant-like and product-like diabatic curves for the concerted synchronous two-bond process (Ia to Ib). Note that the diabatic curves MUST coincide at the geometry of the products and the reactants for the concerted mechanism. This is not the case in Figure 2 of ref 1 but must be the case for the two-bond reaction considered in this paper since the reactants and products of the two-bond concerted reaction are the same. The curves A′/B′ for the two-step reaction must terminate on the product side of the diagram at different points (Z′/Y′) from the concerted process (Z/Y) since the initial product of the two-step reaction is the diradical intermediate Ic. Of course, there will be a second barrier in the two-step, one-bond process corresponding to the formation of the second bond going from Ic to Ib. However, the HL bond eigenfunctions Ib and Ia correspond to the same spin coupling, and thus this barrier will be of conformational origin (a simple rotational potential) and will not be expected to be rate-determining. This observation is in contrast to the conjecture in ref 1 where a second diabatic intersection (of unexplained origin) is assumed for the second step of the nonconcerted process. As we shall presently show, our conjecture is supported by numerical results.

Our task is now to justify the details of the shapes of the diabatic curves shown in Figure 1. We begin with the simplest qualitative arguments and then progress to a more detailed argument based

(8) Bernardi, F.; Olivucci, M.; Robb, M. A.; Tonachini, G. *J. Am. Chem. Soc.* **1986**, *108*, 1408.
(9) Bernardi, F.; Bottoni, A.; McDouall, J. J. W.; Robb, M. A.; Schlegel, H. B. *Faraday Symp. Chem. Soc.* **1984**, *19*, 137–147.
(10) Epiotis, N. D. *Lecture Notes in Chemistry*; Springer-Verlag: New York, 1983; Vol. 34.
(11) Brandow, B. *Adv. Quantum Chem.* **1977**, *10*, 187.
(12) Coulson, C. A.; Fisher, I. *Phil. Mag.* **1949**, *40*, 386.

upon the semiempirical HL valence bond scheme. In a later part of the paper, these arguments are substantiated with the results of numerical computation for specific examples.

We begin by observing that the product-like diabatic is more attractive for the synchronous concerted two-bond reaction (curve D) than for the one-bond reaction (curves B/B'). This fact is immediately apparent from the fact that, at a given point on the reaction coordinate, two partly formed bonds must always have a lower energy than one partly formed bond. Similarly, the reactant-like diabatic must be more repulsive for the synchronous two-bond concerted reaction (curve C) than for the one-bond reaction (curves A/A'). Again, this observation arises from the fact that the energy of two partly broken bonds in the reactant-like diabatic associated with the concerted two-bond process must always be higher that the energy associated with the one-bond process where the two reactant bonds will not have broken to the same extent. However, the interfragment distance will be shorter for the one-bond process than for the two-bond process (i.e., the transition structure for the one-bond process has a smaller interfragment separation). Thus, the two opposing effects will cancel approximately. As a consequence, we are led to the conjecture (see Figure 1) that the intersection point of the reactant-like and product-like diabatic curves is predicted to be at a similar value of the energy. It would thus appear that the magnitude of the resonance interaction between the reactant-like and product-like diabatic curves may control the mechanistic preference for a one-bond or two-bond mechanism.

We must emphasize that the very different behavior of the diabatic surfaces as shown in Figure 1 of the present work when compared with Figures 2 and 3 of ref 1 arises from the fact that we have recognized the requirement that the diabatic curves B and D or A and C must have common end points.

We now extend the preceeding qualitative discussion by using the methodology of semiempirical HL-VB theory. We reemphasize that these arguments will be further substantiated for specific examples using rigorous numerical computation. In the semiempirical HL-VB method (for a modern critical discussion, the reader is referred to the standard textbook[13] of McWeeny and Sutcliffe, Chapter 6), one uses the energy expressions of the various HL-VB configurations as though the orbitals that are used to construct the HL configurations were orthogonal. The exchange integrals, K_{ij}, that occur in the resulting energy formulas are then replaced by the Heitler–London expression (eq 1) for a single bond

$$K_{ij} = [ij|ij] + 2S_{ij}[i|h|j] \quad (1)$$

allowing for the nonorthogonality of the orbitals where the square of the overlap which occurs in the denominator of the HL expression has been neglected. As we shall presently discuss, our numerical implementation of HL-VB scheme using an effective Hamiltonian needs no such approximations. Of course, the rigorous expressions for the matrix elements between HL-VB bond eigenfunctions built from nonorthogonal orbitals involve powers of the overlap, and the approximation just discussed is consistent with keeping only those terms where one neglects all terms where the overlap occurs with a higher power than 1. Clearly, the second term in eq 1 will be negative and large in magnitude relative to the first. While these approximations are not adequate for detailed numerical computation, at this stage we are interested in qualitative arguments only, and this approach should give us an estimate of the dominant effects.

The matrix element expressions for the HL bond eigenfunctions are given in the original paper of Evans,[3] and a detailed discussion is to be found in the textbook of McWeeny and Sutcliffe.[13] The diagonal matrix element (energy associated with a single HL bond eigenfunction) is given as

$$\mathcal{H} = Q + \underset{\substack{\text{spin}\\\text{coupled}}}{\textstyle\sum_{ij}K_{ij}} \quad \underset{\substack{\text{uncoupled}\\\text{spins}}}{-\tfrac{1}{2}\textstyle\sum_{ij}K_{ij}} \quad (2)$$

(13) Mcweeny, R.; Sutcliffe, B. *Methods of Quantum Mechanics*; Academic: New York, 1969.

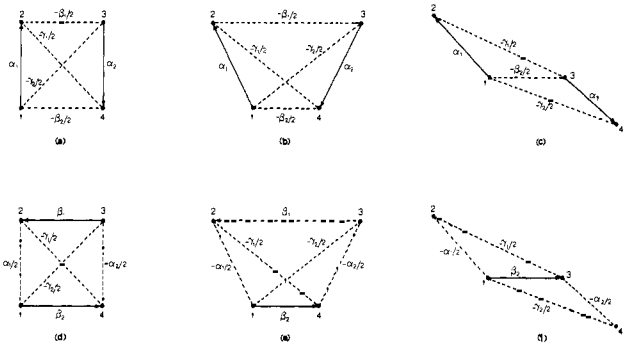

Figure 2. Diagrammatic representation of the formula (eq 2 in text) for the energies of reactant-like (a–c) and product-like (d–e) diabatic states.

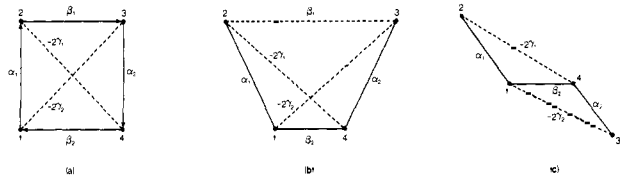

Figure 3. Diagrammatic representation of the formula (eq 3 in text) for the resonance interaction.

and the interaction (resonance) between two HL bond eigenfunctions is given by superimposing the structures of, for example, Scheme Ia/Ib and evaluating eq 3. In these expressions, Q is

$$\mathcal{H} = S[Q + \underset{\substack{\text{odd number}\\\text{of links}}}{\textstyle\sum_{ij}K_{ij}} - \underset{\substack{\text{even number}\\\text{of links}}}{2\textstyle\sum_{ij}K_{ij}} - \underset{\substack{\text{different}\\\text{islands}}}{\tfrac{1}{2}\textstyle\sum_{ij}K_{ij}}] \quad (3)$$

the Coulomb integral and is assumed to incorporate the effects of the repulsions of the doubly occupied orbitals and the nuclear repulsions as well as the small effects arising from the singly occupied valence orbitals themselves. The K_{ij}'s are the exchange integrals and are assumed to be evaluated from eq 1. The overlap integral S is a simple function of the spin coupling.[13] In the H_2 molecule, Q varies only slowly, showing a shallow minimum at the normal internuclear distance, but K_{ij} becomes large and negative and accounts for over 90% of the binding energy of the molecule. For general molecular systems, Q will be dominated by the repulsions of the doubly occupied orbitals (i.e., those not involved in the bond making/breaking process) and the nuclear repulsions. Thus, the behavior of Q will be cosistent with simple steric repulsion arguments. The precise definition of "links" and "islands" is discussed in ref 13. We shall not discuss the details of eq 2 and 3; rather we will be content with an example that is relevant to the present work.

We have illustrated the matrix elements (eq 2 and 3) for the particular bond eigenfunctions of Scheme Ia and Ib/Ic in Figure 2 (diabatic energies) and Figure 3 (resonance interaction). We use α_i to denote the exchange integral (eq 1) involving the AO of the reactant bonds and β_i to denote the corresponding exchange integral for the AO in the product bonds. γ_i is the exchange integrals of the nonbonded AO interactions. In Figures 2 and 3, we have used solid lines for the positive stabilizing interactions (K is negative) and dashed lines for the negative destabilizing interactions. Note that the negative destabilizing interactions occur with a factor of $^1/_2$ in Figure 2, and the nonbonded contributions to the resonance interaction occur with a factor of −2 in Figure 3. The matrix elements for the reactant-like diabatics (Figure 2a–c) and product-like diabatics (Figure 2d–f) are images of each other (aside from the numerical factors of $^1/_2$) in the sense that a stabilizing interaction in the reactant-like diabatic energy becomes destabilizing in the product-like diabatic energy.

We can now rationalize the shapes of the curves in Figure 1 by using simple qualitative arguments based upon the matrix elements of Figures 2 and 3. We need only assume that each interaction ($Q + K_{ij}$) has approximately the form of a Morse potential[3] (i.e., the expressions of eq 1 have the same form as in the HL expression for the hydrogen molecule). Let us consider

first the reactant-like diabatics (Figure 2, parts a, b, and c corresponding to two-bond concerted, one-bond concerted, and one-bond nonconcerted). At a given value of the reaction coordinate, the magnitude of α for Figure 2a (two partly broken bonds) is expected to be smaller than in Figure 2b and c since the 12–34 bonds will be shorter in the later case. However, this effect should be small, and one expects that the values of α should be similar in the various cases. Thus, we expect that the relative shape of the curves is controlled primarily by the destabilizing β and Q. If we compare part a of Figure 2 with parts b and c, we see that the interaction β_1 will fall to zero in parts b and c. Similarily, Q will be less repulsive for the one-bond process (for the same interfragment separation). Furthermore, the nonbonded interactions γ will be smaller in magnitude for Figure 2b and 2c. Consequently, the reactant-like diabatic curve for the nonconcerted one-bond reaction should lie below that for the concerted two-bond reaction, while the diabatic curves for the two one-bond processes should be very similar.

If we examine the matrix elements for the product-like diabatics shown in Figure 2d–f, we see that they are the images (aside from the numerical factors of $^1/_2$) of the interactions of Figure 2a–c in the sense that all the interactions have the same magnitude but opposite sign (except for the nonbonded interaction γ). Thus, we expect the product-like diabatic to be more attractive for the two-bond concerted process (Figure 2d) than for the nonconcerted one-bond process (Figure 2f) primarily because β_1 will be zero for the nonconcerted one-bond process and similarly for the concerted one-bond process.

Thus, as discussed previously, we expect that the fact that the one-bond transition structure occurs at a smaller interfragment separation than the two-bond transition structure and the fact that the stabilizing/destabilizing effects are similar but opposite in sign for reactant-like and product-like diabatics will lead to the result that the energy corresponding to the intersection of the diabatics will be similar for one-bond and two-bond transition structures. We shall later demonstrate by numerical calculation that this is indeed the case.

We now turn our attention to the resonance interaction. The matrix elements (eq 3) are given symbolically in Figure 3. Note that for the resonance interaction the signs of α and β are both positive. If we compare Figure 3a with Figure 3b and c we see that since β_1 is approximately 0 in Figure 3c, we expect that the resonance interaction for the two-bond concerted process will be larger than those for the one-bond processes. We are thus led to a conclusion which is different from that of Dewar[1] for two-bond additions:

The concerted synchronous two-bond and one-bond mechanisms for two-bond cycloadditions are expected to be competitive. This will be the case because the diabatic surfaces are expected to intersect at approximately the same value of the energy. The mechanistic preference should therefore be controlled by the resonance interaction. Therefore, one must expect a small preference for the synchronous mechanism by virtue of the larger resonance interaction in this case.

The preceeding arguments have ignored the consequences of symmetry. We must now consider the consequences of molecular symmetry. In the Woodward–Hoffmann approach, one uses MO's that are adapted to the point group that persists along the reaction coordinate. In the HL-VB approach, the orbitals are not symmetry-adapted, so that the symmetry arguments are not so obvious. In the VB method one must symmetry-adapt the VB configurations rather than the AO. (The principles are discussed for benzene in the text of Eyring et al.[14]) One then constructs the diabatic wave functions from those VB configurations that belong to totally symmetric irreducible representations of the point group that persists over the reaction coordinate. For our purposes, it will be sufficient to consider a point group that consists of at most two generators; the symmetry operation RR that leaves the reactants invariant (if it exists) and the symmetry operation RP

(14) Eyring, H.; Walter, J.; Kimball, G. *Quantum Chemistry*; Wiley: New York, 1944.

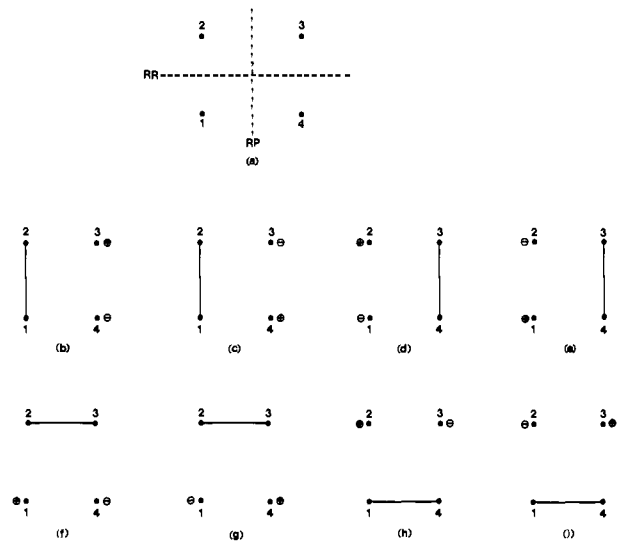

Figure 4. Symmetry elements (RR and RP) for a two-bond cycloaddition (a) and singly ionic charge-transfer configurations (b–i) that can be used to construct symmetry-adapated linear combinations of eq 5a and 5b in text.

that transforms one reactant into the other (if it exists). For the concerted cycloaddition of two ethylenes, RR and RP can be taken as 180-deg/rotations; for the nonconcerted one-bond cycloaddition of two ethylenes to form the tetramethylene trans diradical, only RP (a 180-deg rotation) exists, while for the concerted two-bond Diels–Alder reaction only RR (a reflection plane) exists. We now proceed to show that simple symmetry arguments indicate that the resonance interaction will be approximately one-fourth of its value in the absence of symmetry if both RR and RP are present and one-half of its value in the absence of symmetry if only one of the elements RR or RP is present. Of course one expects this conclusion to hold also if the symmetry is perturbed slightly by substituents.

As we have indicated, in the HL approach with distorted AO, the effects of charge transfer manifest themselves in the delocalization and nonorthogonality of the orbitals. By use of second-order perturbation theory, it is possible to show[11] that the resonance interaction can be written as

$$(\mathcal{H}^{\text{eff}})_{\text{RP}} = \sum_i Z_{\text{R}i} Z_{\text{P}i}/(E_{\text{R}} - E_i) \qquad (4)$$

where Z is the matrix element between the HL configuration (R and P) built from the orthogonal undistorted AO and a charge-transfer configuration (i). $\mathcal{H}^{\text{eff}}$ is an effective Hamiltonian defined in the space of the HL functions which will be discussed in some detail in the next subsection. The HL functions will always be totally symmetric; thus, only symmetry-adapted charge-transfer configurations that are totally symmetric can contribute to $(\mathcal{H}^{\text{eff}})_{\text{RP}}$. We expect that the major contribution to $(\mathcal{H}^{\text{eff}})_{\text{RP}}$ will arise from singly ionic configurations shown in Figure 4. The symmetry operations RR and RP are shown in Figure 4a. The singly ionic charge-transfer configurations associated with the reactant-like diabatic are shown in Figure 4b–e and those for the product are given in Figure 4f–i. If we assume that both RR and RP exist, then only one totally symmetric combination is possible for reactant/product diabatic (eq 5). When the sum in eq 4 is

$$A_1^{\text{R}} = \tfrac{1}{2}(b + c + d + e) \qquad (5a)$$

$$A_1^{\text{P}} = \tfrac{1}{2}(f + g + h + i) \qquad (5b)$$

carried out for these symmetry-adapated functions (i in eq 4), one obtains the same matrix element contributions as in Figure 3 except that the overall result is multiplied by $^1/_4$. When only RR or RP is present, the symmetry-adapted configurations consist of only two terms multiplied by $1/2^{1/2}$; thus, the overall magnitude of $\mathcal{H}_{\text{RP}}^{\text{eff}}$ is $^1/_2$ of its value in the absence of symmetry. These very simple symmetry arguments must of course affect the reactant

and product diabatic curves as well in the sense that the values of E_P and E_R must be correspondingly reduced. However, it can be seen from Figure 2a–c and d–f that these curves are affected in a complementary way so that the conclusion that the one-bond and two-bond diabatics intersect at the same height is not affected. Thus, the main effect of symmetry arguments is on the resonance interaction. One expects that the magnitude of the effect of symmetry on the resonance interaction will be much greater than the small differences in the exchange integrals discussed previously. In general where molecular symmetry is present, the RR symmetry element is missing from the one-bond process but is present in the two-bond process (while the RP element if it exists is present in both). For example, in the two-bond supra–supra cycloaddition (D_{2h} symmetry) of two ethylenes, the 180-deg RR operation, which is present for this case, disappears in the one-bond nonconcerted (C_{2h} symmetry) approach, while the RP symmetry operation is present for both. Thus, in the case where the RR symmetry operation exists for the concerted two-bond reaction, the one-bond reaction (either concerted or nonconcerted) where RR does not exist will be preferred due to the magnitude of the resonance interaction (which according to the above discussion will be about twice as large in the one-bond process). In summary, the arguments that neglect symmetry favor the two-bond mechanism because of the resonance interaction. On the other hand if the RR symmetry element exists for the two-bond process, the resonance interaction for the two-bond concerted reaction will be approximately one-half of the value for the one-bond process.

In conclusion, we must add a note of caution. The preceeding arguments are implicitly based on the assumption that the interaction of the diabatic surfaces via the resonance interaction produces a transition structure saddle point surface. While this seems obvious in a two-dimensional space, this may not always be true. The nature of the resonance interaction may be such that, at the minimum of the seam of intersection of the diabatic surfaces, after the interaction is "switched on" no saddle point surface (and thus no transition structure) exists. In our study of the concerted and nonconcerted cycloaddition of two ethylenes,[7] at the 4-31G basis set level, the diradical minimum (for the nonconcerted one-bond process) has a barrier to fragmentation of less than 1 kcal/mol. Similarily, in our calculations on the Diels–Alder reaction,[15] the diradical minimum/one-bond transition structure did not exist at the 4-31G level. Thus, while the preceeding arguments predict, for example, that the one-bond asynchronous mechanism for the Diels–Alder is preferred (by virtue of the symmetry effects on the resonance interaction), there is no guarantee that a transition structure for this process actually exists. Only a full geometry search can answer this question. Thus, in our numerical computations which follow, we are limited to showing that the preceeding arguments are valid for particular examples where the transition structures have been documented.

3. Rigorous Implementation of the Diabatic Surface Model

We shall now describe briefly how the scheme discussed above can be implemented in the context of the MC-SCF method that has been used to optimize the geometries to be considered in several examples. We shall be content with only a brief summary of the main ideas since the method has been fully documented elsewhere.[4b,c]

We now consider a similarity transformation of the full CI Hamiltonian for four electrons in four orbitals (Scheme II). We have partitioned the full CI space into a block spanned by the reference configurations R and P and a secondary block spanned by the remainder of the configurations. We now seek the transformation matrix **U** which reduces the full CI Hamiltonian (left-hand side of Scheme II) to the blocked form (right-hand side of Scheme II) where the interaction matrix elements between R and P and the remainder of the configurations are zero. The eigenvalues of the submatrix H^{eff} (an effective Hamiltonian matrix) corresponding to the right-hand side of Scheme II will

Scheme II

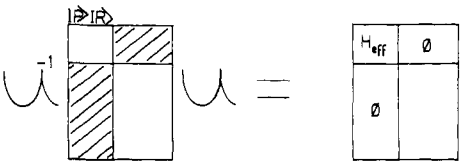

now reproduce two eigenvalues (and thus two adiabatic surfaces) of the original Hamiltonian matrix exactly. Thus, the diagonal elements of $\mathbf{H}^{eff}$ are the diabatic surface energies, the off-diagonal element is the resonance interaction, and the Pth and Rth columns of **U** give the wave functions for the diabatic surfaces of reactant and product. In our work we have used the canonical Van Vleck[16–19] method to compute the transformation **U**.

We now give some particulars of the implementation and interpretation of this scheme in the present context. The Hamiltonian which appears on the left-hand side of Scheme II is constructed from configurations used in a four-orbital, four-electron CAS MC-SCF where the converged MOs have been subsequently localized onto the atomic centers. Thus, the space of the full Hamiltonian on the left-hand side of Scheme II corresponds to a full VB space where the configurations have been constructed from orthogonal atom-localized orbitals. The coefficient vector (diabatic wave function) corresponding to the Pth or Rth column of the transformation matrix **U** will be dominated by the corresponding Pth or Rth component corresponding to the configurations of Scheme Ia or Ib with much smaller contributions from charge transfer, etc. The effective Hamiltonian which appears on the right-hand side of Scheme II corresponds to the projection of the full VB Hamiltonian onto the space of the configurations of Scheme Ia and Ib/c. Thus, the effective Hamiltonian is the Hamiltonian of the HL-VB space where the configurations have been constructed from distorted nonorthogonal orbitals (resulting from the charge-transfer configurations that appear in the transformation matrix **U**). A second-order perturbation estimate of the off-diagonal elements of the effective Hamiltonian is given in eq 4 and the magnitude of the resonance interaction is thus determined mainly by charge-transfer effects (the zeroth-value being very small) or equivalently the resonance interaction results from the distortion and overlap of the atomic orbitals (as in the MO treatment of benzene).

At this point we need to give a very brief discussion of the spin coupling that is used in numerical calculations. We shall limit our discussion to the four-orbital/four-electron case used in these examples: for a general background the reader is referred to the book by Pauncz.[20] For interpretive purposes, the Rumer bond eigenfunctions are the obvious choice of CI basis in which to formulate our discussion of bonding interactions. However, for computional purposes, the orthogonal Yamanouchi–Kotani basis is usually used.[16] The Yamanouchi–Kotani basis is obtained from the Rumer basis by Schmidt orthogonalization (see the book by Pauncz[16] for details). However, the simple physical interpretation of the Rumer basis could be retained by some other orthogonalization procedure (such as symmetric orthogonalization). This in turn merely corresponds to an orthogonal transformation of the Yamanouchi–Kotani basis. Nevertheless, the product-like Rumer function is identical with the Yamanouchi–Kotani spin function if the Schmidt orthogonalization is started with this function, while the reactant-like Rumer function is obtained by starting the orthogonalization with this function. It is thus apparent that in the Yamanouchi–Kotani basis the spin coupling must be allowed to "rotate" through an angle of 30° as a function of the reaction coordinate (since the overlap of the Rumer functions is one-half, Schmidt orthogonalization corresponds to

(15) Bernardi, F.; Bottoni, A.; Robb, M. A.; Field, M. J.; Hillier, I. H.; Guest, M. F. *J. Chem. Soc., Chem. Commun.* **1985**, 492.

(16) Van Vleck, J. H. *Phys. Rev.* **1929**, *33*, 467.
(17) Jordahl, O. M. *Phys. Rev.* **1934**, *45*, 87.
(18) Kemble, E. C. *Fundamental Principles of Quantum Mechanics*; McGraw-Hill: New York, 1937; p 394.
(19) Shavitt, I.; Redmon, L. T. *J. Chem. Phys.* **1980**, *73*, 5711.
(20) Pauncz, R. *Spin Eigenfunctions*; Plenum: New York, 1979.

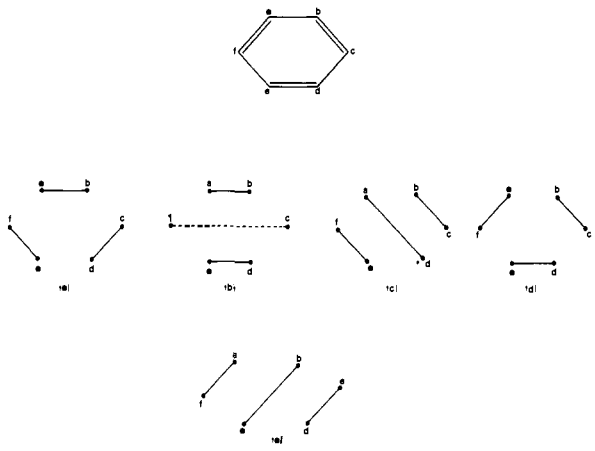

Figure 5. Bond eigenfunctions for a (4 + 2) cycloaddition reaction. In a four-orbital representation, a and b are used with the ab pair doubly occupied. In a six-orbital representation, the main additional contribution arises from d.

rotation of one of the Rumer functions by 30°). However, since we know the transition structure geometry, we simply choose the spin coupling at the transition structure geometry so that the two diabatic surfaces intersect exactly at the transition structure geometry in order to avoid this rather arbitrary rotation.

In the calculations to be discussed subsequently, we shall treat all two-bond addition reactions as four-orbital/four-electron problems in both the MC-SCF and (via the Van Vleck transformation just discussed) the HL-VB formalisms. While for a (2 + 2) cycloaddition this is the only possibility; for a (4 + 2) cycloaddition the situation is less obvious, and some justification is required to avoid confusion with traditional VB methods. If we take the Diels–Alder reaction or a 1,3-dipolar cycloaddition as an example, then the argument becomes clear. On the one hand, each reaction involves the making/breaking of two bonds so that four active orbitals (i.e., orbitals that may have other than double occupancy) and four electrons are involved. Thus, an MC-SCF with four orbitals and four electrons will be adequate to describe the transition structure region. On the other hand, by analogy with the VB picture of resonance in benzene, one might be lead to expect that, because one needs five HL configurations for six electrons in six orbitals to describe the resonance energy, a six-orbital/six-electron active space might be required to describe the transition structure and the diabatic surface intersection. (This picture of resonance was the one used by Evans.[2,3]) In fact, a six-active-orbital/six-electron space is not required within the formalism we use, since as in benzene in an MO description the resonance effect manifests itself in terms of the delocalization of the AO to form a MO. We now discuss this argument in more detail.

In Figure 5 we give the five HL structures for six electrons in six orbitals. For the Diels–Alder problem, the ab pair corresponds to the middle pair of carbon atoms of butadiene, while for a 1,3-dipolar cycloaddition the ab pair corresponds to the lone pair on the central atom of the 1,3 dipole. In a four-orbital/four-electron model, the two HL configurations required to describe the transition structure are configurations of Figure 5a and b where the ab pair remains spin-coupled (i.e. is a "passive" doubly occupied core orbital). In the six-electron representation, the configuration of Figure 5d will interact with both of the configurations of Figure 5a and b. We expect that the configurations of Figure 5c and e will be negligible. At first sight these two pictures seem unrelated. However, the effect of the interaction of the configurations of Figure 5a and b with Figure 5d is merely to delocalize the orbitals f and c onto the centers a and b. On the other hand, one could also obtain the four-electron model from the six-electron model by using the Van Vleck transformation just discussed and projecting the six-active-orbital CI Hamiltonian onto the space of the four-active-orbital space of configurations of Figure 5a and b. Again, the effect of the configuration of Figure 5d would be equivalent to a delocalization of the AO f and c onto the centers

Scheme III

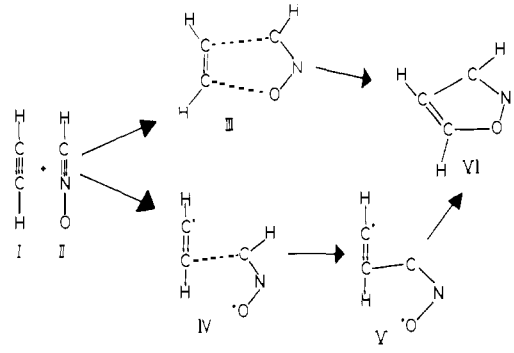

a and b. Of course, the numerical results for a six- and four-electron treatment will be different for the same reason that the VB and MO methods give different results for the resonance energy of benzene (i.e., the six-orbital/six-electron VB treatment spans a variational space which is larger than the single configuration MO space). In our method we localize the four active orbitals onto atomic centers. If these active orbitals involve only the centers c–f, then the orbitals will only localize on these centers. On the other hand, if the four active orbitals involve contributions from centers a and b, then the resultant atom-localized AO will have "delocalization tails" on centers a and b. This result is determined by the nature of the MC-SCF orbitals. Thus, the need to describe the making/breaking of two-bonds determines the number of active orbitals, and hence the use of four active orbitals for two-bond reactions should be adequate. In the subsequent decomposition using atom-localized AOs in configurations of Figure 5a and b, the effect of the configuration of Figure 5d is to delocalize the c and f AOs onto centers a and b. In our recent study[15] of the Diels–Alder reaction, the interfragment distance was changed by only 0.04 Å at the transition structure by the change from four to six active electrons. Further, in our four-electron MC-SCF calculations, the middle ab pair was localized with negligible contributions from atoms f and c (Figure 5). Thus, in our discussion of (4 + 2) cycloadditions, we shall be concerned with the resonance interaction between HL configurations a and b of Figure 5. The effect of the configuration of Figure 5d is in fact implicitly included in this treatment and manifests itself as a delocalization of the orbitals f and c onto the a–b bond.

All computations presented in this work have been performed at the STO-3G level[21] using MC-SCF codes[22,23] that have been incorporated into the GAUSSIAN 80 suite[24] of programs. We have demonstrated in previous work that the topological features (number and nature of minima and transition structures) of the potential energy surfaces we shall study are in agreement at STO-3G and 4-31G levels[6,7,9] (although the geometries and magnitude of energetic effects are obviously quite different).

4. Results and Discussion.

In this section we will consider three examples that illustrate the ideas that we have considered previously.

(i) **1,3-Dipolar Cycloaddition of Acetylene to Fulminic Acid. Concerted vs. Two-Step Mechanism.** Recently[9] we have located (at the MC-SCF level by using STO-3G and 4-31G basis sets) the transition structures (III and IV) and diradical intermediates (V) for the addition of acetylene (I) to fulminic acid (II) (Scheme III). Our calculations[9] show that the concerted transition state (III) is lower than the nonconcerted transition state (IV) by 5 kcal/mol at the 4-31G level (7 kcal/mol at STO-3G) and that the barrier for the second stage of the reaction (V to VI) lies below III or IV. In ref 25, the opposite conclusion was reached, namely

(21) Hehre, W. J.; Stewart, R. F.; Pople, J. A. *J. Chem. Phys.* **1969**, *51*, 2657.
(22) Eade, R. H. A.; Robb, M. A. *Chem. Phys. Lett.* **1981**, *83*, 362.
(23) Schlegel, H. B.; Robb, M. A. *Chem. Phys. Lett.* **1982**, *93*, 43.
(24) Binkley, J. S.; Whiteside, R. A.; Krishnan, R.; Seeger, R.; De Frees, D. J.; Schlegel, H. B.; Topiol, S.; Kahn, L. R.; Pople, J. A. *QCPE* **1981**, *13*, 406.

Table I. Diabatic Energies (in au) Evaluated at the Transition Structure Geometries (III and IV) for the 1,3-Dipolar Cycloaddition of Fulminic Acid (II) to Acetylene

	III (r_{C-C} = 2.37 Å)	IV (r_{C-C} = 2.12 Å)
diabatic energy for product-like reactant-like surface	−241.1922	−241.2003
resonance interaction	−0.1134	−0.0947
adiabatic energy	−241.3056	−241.2950

that the nonconcerted path was favored. However, in ref 25 the methods used were not able to treat the concerted and nonconcerted pathways on an equal footing as in the MC-SCF results reported in ref 9. The sensitivity of the results in ref 25 to the inclusion of dynamic electron correlation may be an artifact of this unbalanced description.

When the two bonds that are formed in a pericyclic reaction are different (as in the present case where a C–C and a C–O bond are formed), it is difficult to assess clearly whether a concerted process should be called synchronous or asynchronous. The process might be synchronous with respect bond length yet asynchronous with respect to bond strength because of different stretching potentials for the two newly formed bonds. However, as discussed in ref 20 of ref 25, the assignment of diagonal force constants for the C–C and the C–O stretches is dependent upon an arbitrary choice of internal coordinates in the case of cyclic molecules. For this reason it is preferable to use a criterion based on the extent of new bond formation as a criterion for assessing whether a concerted process is synchronous or asynchronous. If we take R, the bond length in the product, as the reference and denote the bond length in the transition structure by r, then the extent of new bond formation is given by $S = R/r$. For the concerted transition structure III, the values of S are 0.64 (0.60) and 0.62 (0.66) for the C–O and C–C bonds, respectively, at the STO-3G (and 4-31G) level.[9] According to this criterion, the concerted process is synchronous, and we have a situation where a concerted synchronous two-bond reaction appears to be preferred over the first step of the two-step process.

We now attempt to rationalize this behavior by using the diabatic surface method which has been discussed in the previous section. Fulminic acid (II) can be thought of as having two allyl-like systems of three π-orbitals: an in-plane π set and an out-of-plane π set (incipient delocalized π-orbitals). Similarly the acetylene has two sets of ethylene π-orbitals: an in-plane set and out-of-plane set. In our MC-SCF calculations, we take as active orbitals the HOMO–LUMO pair for the in-plane set of fulminic acid orbitals and the corresponding acetylene in-plane orbitals. The MC-SCF orbitals are then localized by using an intrinsic energy localization procedure. The resultant orbitals are localized on the C and O atoms of the fulminic acid and the C atoms of the acetylene. With this choice of orbitals, we have computed the first and second derivatives of each diabatic surface. In ref 26 this procedure has been tested by finding the minimum of the seam of intersection of the two diabatic surfaces in this type of quadratic representation. The "diabatic transition structure" so obtained is very close to the true adiabatic transition structure. In order to convey this representation of the diabatic surfaces in a simple way, the first and second derivative information has been projected onto the transition vector (eigenvector of the adiabatic second derivative matrix corresponding to the direction of negative curvature) and the resulting one-dimensional quadratic information plotted against the interfragment C–C bond length. These curves have then been "continued" to the corresponding product geometries.

The results are collected in Figure 6, and the numerical data are summarized in Table I. Curves C and D represent the diabatic surfaces for the reactant (Scheme Ia) and the product

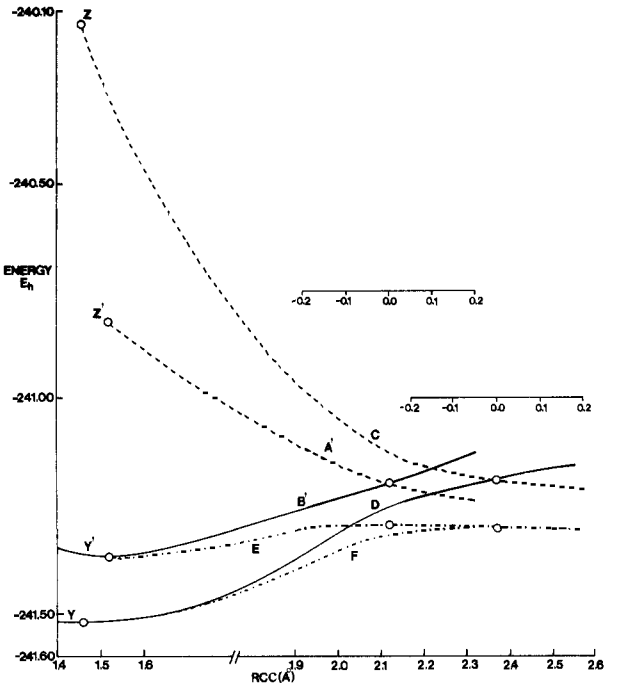

Figure 6. Diabatic curves for the 1,3-dipolar cycloaddition of fulminic acid (II) to acetylene (I) forming isoxazole (VI). (A′) Reactant-like diabatic curve for the first step of the two-step process (I + II to V via IV). (B′) Product-like diabatic curve for the first step of the two-step process (I + II to V via IV). (C) Reactant-like diabatic curve for the concerted synchronous process (I + II to VI via III). (D) Product-like diabatic curve for the concerted synchronous process (I + II to VI via III). (E) Adiabatic curves for the first step of the two-step process (I + II to V via IV). (F) Adiabatic curves for the concerted synchronous process (I + II to VI via III).

(Scheme Ib) for the concerted synchronous process (I + II going via III to VI). Similarly curves A′ (Scheme Ia) and B′ (Scheme Ib) represent the analogous result for the first step (I + II going via IV to V) of the two-step process. Curves E and F are the adiabatic energies represented in the same way as the diabatic energies. Finally Y/Y′ and Z/Z′ represent the continuation of the curves D and B′ or C and A′ to the minima V and VI.

Curves C and D of Figure 6 should be compared with the correspondingly labeled, qualitative results of Dewar to be found in Figure 2 of ref 1 and the qualitative curves given in Figure 1 of the present work. Similarily curves A′ and B′ of Figure 2 should be compared with curves A and B of Figure 3 of ref 1 and A′ and B′ of Figure 1 of the present work.

It can be seen that the computed diabatic curves (shown in Figure 6) have the expected qualitative behavior in agreement with our earlier qualitative predictions (but in disagreement with ref 1 for reasons discussed above). From these computed results one observes that (a) the reactant-like diabatic is more repulsive for the concerted synchronous reaction (curve C) than for the first step of the two-step (curve A′) reaction and (b) the product-like curve is more attractive for the concerted synchronous reaction (curve D) than for the first step of the two-step (curve B′) reaction.

These two effects partly cancel with the result that the height of the intersection is almost the same for both processes. The resonance interaction $(\mathcal{H}^{\text{eff}})_{RP}$ (difference between the intersection point and the adiabatic energies) thus plays the deciding role. The difference between the heights of the intersection points is 5 kcal/mol, with the nonconcerted one-bond intersection being lowest in energy. On the other hand, the resonance interaction for the two-bond concerted process is 11.7 kcal/mol larger than for the nonconcerted process. This is consistent with the fact that the barrier height for the concerted two-bond process is only 6.7 kcal/mol (4.7 kcal/mol at the 4-31G level) lower than for the nonconcerted process. Thus, the concerted process is favored by the resonance interaction in agreement with the qualitative discussion given previouslv.

(25) Hiberty, P. C.; Ohanessian, G.; Schlegel, H. B. *J. Am. Chem. Soc.* **1983**, *105*, 719.
(26) McDouall, J.; Robb, M. A.; Bernardi, F. *Chem. Phys.* Lett. **1986**, *129*, 595.

Scheme IV

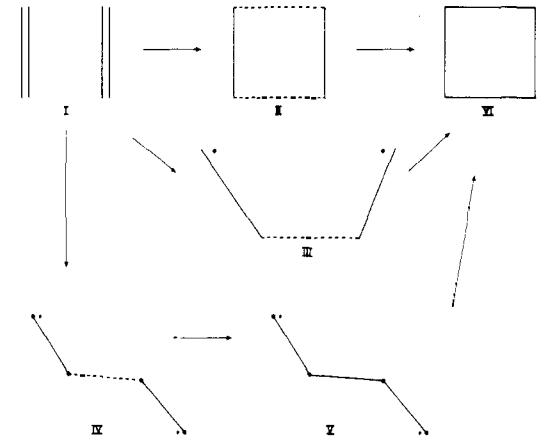

Table II. Diabatic Energies (in au) for the Cycloaddition of Two Ethylene Molecules

	supra–supra concerted two bond	cis (coplanar) concerted one bond	trans nonconcerted one bond
diabatic energy for reactant/product	−154.0728	−154.0694	−154.0732
resonance energy	0.0545	0.0967	0.1018
adiabatic energy	−154.1273	−154.1661	−154.1751

There is one final point that requires some discussion at this point. In our MC-SCF geometry optimizations,[9] we observed that the barrier for the second stage of the reaction (V to VI) lies below III or IV. From Figure 6 it is apparent that the diradical intermediate (V) and the cyclic product (VI) lie in a region of the potential surface that is dominated by the product-like diabatic (Scheme Ib/c). Thus, the second barrier is essentially a rotational potential of low energy and does not arise from a diabatic surface crossing. In his paper,[1] Dewar arrives at a rather different conclusion. In Figure 3 of ref 1, three different diabatic surfaces are used: reactant-like (similar to our work), diradical-like (similar to our product diabatic), and a surface associated with the cyclic product. Dewar[1] then postulates that for many two-step reactions the barrier associated with the intersection of the latter two diabatic surfaces will be larger than that associated with the first two diabatic surfaces. However, as we have previously pointed out, the configuration shown in Scheme Ib/c can describe either two bonds or a single bond and a diradical. Thus, the formation of the second bond from the diradical intermediate involves no electronic reorganization associated with a diabatic surface crossing.

(ii) **Cycloaddition of Two Ethylenes Producing Cyclobutane or the *trans*-Tetramethylene Diradical.** A comparison of the Woodward–Hoffmann forbidden ($2_s + 2_s$) cycloaddition (concerted two bond) of two ethylene molecules (I) yielding cyclobutadiene (VI) via a concerted two-bond transition state (II) or concerted one-bond transition state (III) as opposed to the two-step (one-bond) addition to form the tetramethylene diradical (IV) provides an interesting contrast to the previous example (Scheme IV). In previous work,[7] we have located the stationary points on the potential energy surface for II, III, and IV as well as the various minima. It turns out that the Hessian for II and III has two directions of negative curvature so that only IV is a true transition structure. However, since critical points exist for the two-bond concerted process (II), the one-bond concerted process (III), and the one-bond nonconcerted process (IV), it is of interest to examine the role of the resonance interaction (and the effect of symmetry) in these three mechanisms.

The diabatic surface data are displayed in Figure 7 in the same manner as in the previous subsection and is also collected in Table II. The diabatic curves have the behavior predicted earlier. The intersection point is at a similar value of the energy for the three possible processes. The reactant-like diabatic curve for the

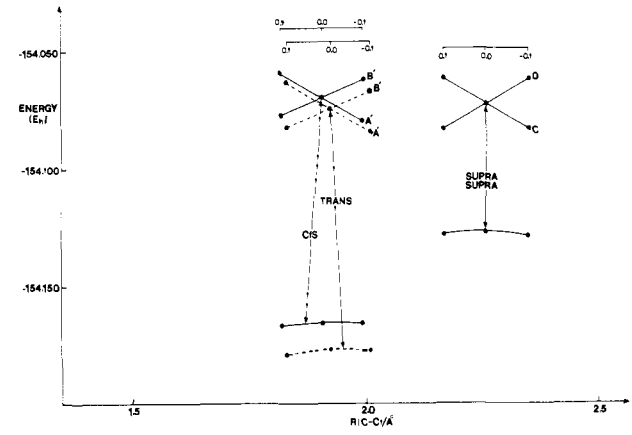

Figure 7. Diabatic curves for the (2 + 2) cycloaddition of two ethylenes.

Table III. Diabatic Energies (in au) for the Addition of H_2 to CO

	transition structure	
	synchronous[a]	asynchronous[b]
diabatic energy for product-like surface	−112.17654	−111.9967
diabatic energy for reactant-like surface	−111.8713	−111.9966
resonance interaction	−0.0623	−0.2044
adiabatic energy	−112.1872	−112.2004

[a] Figure 8 with C_{2v} symmetry. [b] Figure 8.

two-bond concerted process (I–II–VI) is much more repulsive than for the one-bond processes (I–III–VI or I–IV–V), and the product-like diabatic curves have the image behavior. The resonance energy for the two-bond concerted process is much smaller than for the one-bond processes by virtue of symmetry. Thus, the relative energies of the transition structures are controlled mainly by the resonance interaction. As predicted by our qualitative discussion, the resonance interaction of the two-bond concerted process (I–II–III) where RR and RP exist has a value that is about one-half of the value for the one-bond processes (I–III–VI or I–IV–V) where only the symmetry element RP exists. This leads to the fact that the structures III and IV have considerably lower energies than II. Thus, while the topology of the potential surface (the number and nature of the stationary points such as minima and transition structures) is controlled by the diabatic surfaces themselves (as we have demonstrated in previous work[8]), the relative energetics are controlled mainly by the magnitude of the resonance interaction.

In contrast to the previous example of a 1,3-dipolar cycloaddition (Woodward–Hoffmann allowed), in the present example the magnitude of the resonance interaction is determined by symmetry considerations. Further, these symmetry considerations will continue to hold approximately when the system is perturbed slightly (such as by functional group substitution).

(iii) **Addition of H_2 to CO. Concerted Two-Bond Reaction vs. Concerted one-Bond Reaction.** As a final example we consider the addition of H_2 to CO. This process is Woodward–Hoffmann-forbidden in C_{2v} symmetry and takes place by a highly asymmetric transition state of C_s symmetry in which one of the C–H bonds is almost completely formed (our geometry optimization at the MC-SCF level is to be found in ref 23). Thus, it represents an example of a concerted asynchronous reaction. The transition state for a C_{2v} approach occurs at a point where the H_2 moiety is completely dissociated into two H atoms. In order to compare the C_s and C_{2v} approaches, we have performed our C_{2v} computations at a geometry where all the parameters (H–H distance, CO–HH distance) are the same as for the C_s transition structure.

In order to construct the diabatic surfaces for the asynchronous concerted one-bond process, we take orbitals 1 and 2 (Scheme I) to be the carbon lone-pair σ-orbital of CO and the in-plane $p\pi$ atomic orbital of CO, respectively. Similarly for orbitals 3 and 4 (Scheme I), we take the 1s orbitals of H_2 (i.e., we use atom-

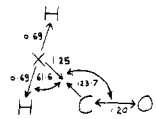

Figure 8. Geometry for the transition structure of H_2 + CO (optimized at the MC-SCF/STO-3G level). The curved arrows give the general form of the transition vector.

Scheme V

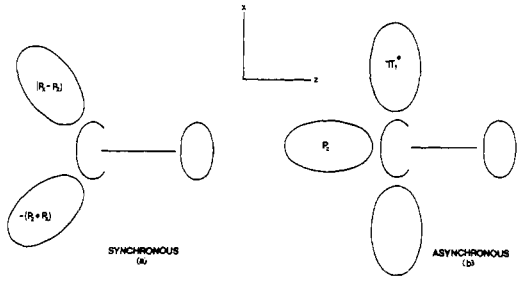

localized AO for H_2; however, for CO we have chosen the two orbitals of the C atom to be canonical). These are illustrated in Scheme Va. For the corresponding synchronous pathway we have used "equivalently" localized orbitals for the C atom (Scheme Vb). For the asynchronous pathway, in Figure 8 we have sketched the form of the transition vector along where the diabatic gradients and second derivatives have been projected for the asynchronous approach. It should be noted that as the distance between the carbon atom and the center of mass of H_2 is decreased, the H–H bond stretches and the angle between the H_2 and the CO opens up. Thus, as one C–H bond is being formed, the other is actually being weakened. For the corresponding concerted synchronous pathway, which leads only to dissociation of H_2 into 2H (i.e., the true C_{2v} transition state occurs at an infinite H–H distance), in order to *simulate* a C_{2v} approach, we have made the projection of the diabatic forces and second derivatives steps along the same transition vector as for the asynchronous pathway keeping the angle with CO fixed at 90° with all other variables the same.

In Figure 9 we have illustrated the projections of the first and second derivatives of the diabatic surfaces in the same manner as for previous examples. For the asymmetric path, A and B represent the product-like and reactant-like diabatics, and the difference between this curve and the adiabatic curve E arises from the resonance interaction, $(\mathcal{H}^{\text{eff}})_{RP}$. Curves C, D, and F represent the corresponding information for this C_{2v} symmetric path.

Before drawing the readers attention to the salient points of these diabatic curves, we should remind the reader that when a concerted synchronous and concerted asynchronous process are compared, the diabatics must coincide at infinite interfragment separation and also at the product geometry. At intermediate geometries the asynchronous path is *curved*, and thus the diabatic and adiabatic surfaces will differ. In Dewar's paper,[1] in Figure 2, he has assumed that the diabatic curves for, say, the product for the concerted synchronous reaction and the concerted asynchronous reaction will coincide only at the product geometry.

Returning to our discussion of Figure 9, on examining curves C and D (product-like and reactant-like diabatics for the C_{2v} synchronous approach), we see that the intersection occurs on the reactant side of the transition state (i.e., at the C_s transition structure geometry, the product-like C_{2v} diabatic curve is considerably lower in energy than the reactant-like C_{2v} diabatic curve). The diabatic surface intersection in the C_{2v} pathway corresponds to two partly formed bonds. However, at the C_s transition state, one bond (C–H_2) is almost completely formed and the intersection corresponds to the intersection of the reactant-like diabatic with a diabatic that is similar to the one-bond product-like diabatic surfaces computed for the one-bond nonconcerted processes considered previously. The resonance interaction, $(\mathcal{H}^{\text{eff}})_{RP}$, at the C_s transition structure is very large (128 kcal/mol) compared to the value at the corresponding point on the C_{2v} pathway (39 kcal/mol) as expected from symmetry considerations. Thus, while the reactant-like diabatic surface for the two-bond synchronous

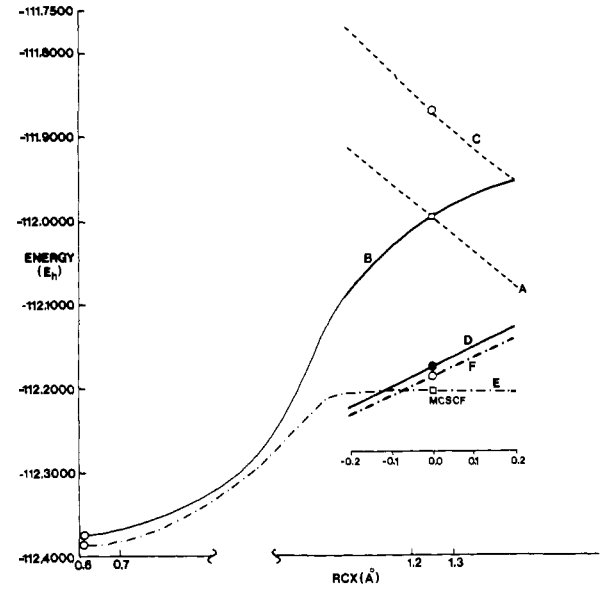

Figure 9. Diabatic curves for the addition of H_2 to CO. (A) Product-like diabatic curve for the asynchronous path. (B) Reactant-like diabatic curve for the asynchronous path. (C) Product-like diabatic curve for the synchronous (C_{2v}) path. (D) Reactant-like diabatic curve for the synchronous (C_{2v}) path. (E) Adiabatic curves for the synchronous path. (F) Adiabatic curves for the asynchronous path.

process is highly stabilized, the very small value of the resonance interaction is not sufficient to allow the diabatic surfaces to interact sufficiently to allow a transition structure to form on the C_{2v} pathway. Clearly, it is the resonance interaction that is critical in the mechanism.

5. Conclusions

In this work we have attempted a qualitative and quantitative study of the diabatic curves used by Dewar[1] in his formulation of selection rules for multibond reactions. In agreement with the conjecture of Evans[2,3] and Dewar,[1] we have illustrated that, for the two-bond reactions studied in this work, the resonance interaction plays a important role in mechanistic considerations in the preference of concerted synchronous (two-bond) vs. concerted/nonconcerted asynchronous (one-bond) reactions. In contrast to Dewar[1] we have illustrated that in a comparison of one-bond vs. two-bond mechanisms, the diabatic curves intersect at approximately the same value of the energy, and thus, the resonance energy can play the deciding role. Thus, while the topology of the potential energy surface appears to be determined by the diabatic surfaces alone[8] (i.e., the transition structures lie on the minima of the seam of intersection), the relative energetics may be determined almost completely by the resonance interaction.

For Woodward–Hoffmann-allowed reactions, qualitative arguments show that a concerted two-bond process may be favored over the nonconcerted one-bond process by virtue of the resonance interaction. This conjecture is illustrated by the example of the Woodward–Hoffmann-allowed reaction of fulminic acid with acetylene. In this example, the magnitude of the resonance interaction is larger at the transition-state geometry corresponding to the concerted synchronous process than at the transition state for the first step of the two-step process. This leads to the fact that the two processes can be competitive in cases such as the one studied here where the reactant-like and product-like diabatic curves intersect at similar heights.

As we have discussed previously, the magnitude of the resonance interaction is reduced if symmetry is present. Further, one expects that the magnitude of this effect will be much larger than the small differences in exchange integrals that lead to the preference for the synchronous two-bond mechanism in the case of the 1,3-dipolar cycloaddition. This argument is illustrated by the calculations on the cycloaddition of two ethylene molecules and the addition of H_2 to CO. Thus, for the cycloadditton of two ethylenes (Woodward–Hoffmann forbidden in a supra–supra approach),

the resonance interaction at the transition structure corresponding to the concerted synchronous process is about one-half (from symmetry considerations since RR is present) its value for the asynchronous one-bond process (where the RR element is not present). In common with the Woodward-Hoffmann approach, one expects that arguments based on symmetry will still hold when the system is perturbed slightly by functional group substitution.

In all our calculations on two-step reactions,[6,9] the diradical intermediate with one bond formed lies on a surface that is dominated by the same product-like diabatic surface as the final cyclic product, and thus, the second barrier to form products is very small.

Of course there is a great debate on the synchronous vs. nonsynchronous nature of cycloadditions (see the discussion in ref 1). We have treated only three examples numerically in this paper. These examples have been chosen because the topology of the potential surfaces is reliably documented at the MC-SCF level where the diradical one-bond transition structure can be determined with the same accuracy as the transition structure for the synchronous path. While the calculations reported in this work have been carried out at the STO-3G level (for reasons of economy), in all of the cases studied the preference for concerted/nonconcerted pathways at the 4-31G is correctly reproduced at the STO-3G level. Thus, while basis set effects appear to be very important in determining the stability of the products relative to the reactants and the barrier heights (see ref 9, for example), the relative energies of the concerted and nonconcerted transition structures appear to be reliable at the STO-3G level. Thus, for these examples, the qualitative arguments of section 2 of this paper have withstood the test of numerical computation.

Finally, we should point out that arguments based upon diabatic surface intersections do not guarantee that the transition structure for one or the other of the possible pathways actually exists. Thus, for ethylene cycloaddition, the minimum and transition structures for the one-bond nonconcerted process virtually disappear for this preferred mechanism. similarily, on the basis of the symmetry arguments presented previously, the one-bond mechanism for the Diels-Alder reaction should be preferred since the RR symmetry element (a reflection plane) is present for the synchronous approach. However, at the MC-SCF 4-31G level no transition structure exists[15] for the one-bond mechanism. In other words, the existence of a minimum of a diabatic surface crossing does not imply that the saddle point surface of the transition structure will actually be formed when the resonance interaction is "switched on". This fact is also demonstrated in the example of the addition of CO to H_2 considered in this work.

In conclusion, we believe that the present results indicate that, while the electronic origin of the reaction barrier[6-9] can be understood from a knowledge of the diabatic surface intersections alone, the resonance interaction plays the dominant role in discriminating between concerted synchronous two-bond and concerted/nonconcerted one-bond reaction mechanisms since the diabatic surfaces for the possible competing mechanisms intersect at similar values of the energy.

Acknowledgment. This work has been supported in part from Grant GR/D/23305 from the Science and Engineering Council of the U.K. and by the EEC under Contract ST2-0083-2-UK.

Registry No. CO, 630-08-0; acetylene, 74-86-2; fulminic acid, 506-85-4; ethylene, 74-85-1.

Thermal Isomerization of Benzocyclobutene

Orville L. Chapman,* Uh-Po Eric Tsou, and Jeffery W. Johnson

Contribution from the Department of Chemistry and Biochemistry, University of California, Los Angeles, Los Angeles, California 90024. *Received June 23, 1986*

Abstract: Thermolysis of benzocyclobutene ($^{13}CH_2$, 99%) gives styrene labeled in the β (48%), ortho (30%), α (14%), meta (4%), and para (4%) positions. The major labels (β and ortho) are consistent with a mechanism involving interconversions of the isomeric tolylmethylenes and the methylcycloheptatetraenes. This mechanism also involves interconversion of *o*-tolylmethylene with *o*-xylylene and *p*-tolylmethylene with *p*-xylylene. A minor mechanism produces 25% of the styrene. This mechanism involves cleavage of the aryl carbon to the methylene carbon bond in benzocyclobutene followed by hydrogen transfer to produce styrene. Thermolysis of *p*-xylylene produced from [2.2]paracyclophane gives styrene (55%), *p*-xylene (31%), benzocyclobutene (4%), benzene (4%), and toluene (3%). Thermolysis of [2.2]metacyclophane gives styrene (18%), *p*-xylene (25%), *m*-xylene (3%), benzocyclobutene (1%), benzene (7%), and toluene (22%).

The thermal isomerization of benzocyclobutene to styrene[1] provides an interesting mechanism problem. The simplest mechanism for this process involves homolysis to a diradical followed by hydrogen transfer (mechanism I). An alternative, mechanism II, involves the interconversions of the tolylmethylenes and methylcycloheptatetraenes established by matrix isolation studies.[2] This mechanism also explains the thermolysis (150 °C) of *o*-tolyldiazomethane to benzocyclobutene and styrene reported by Vander Stouw and Shechter[3] and the thermolysis (420 °C) of *m*- and *p*-tolyldiazomethanes to benzocyclobutene and styrene reported by Baron et al.[4] Mechanism II is consistent with the ^{13}C-labeling experiment of Hedaya and Kent[5] (eq 1) and with the ^2H-labeling experiment of Vander Stouw et al. (eq 2).[6]

mechanism I

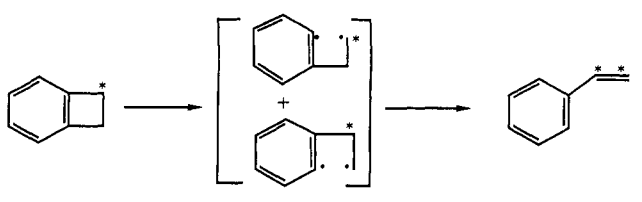

* = ^{13}C

(1) (a) Baron, W. J.; DeCamp, M. R. *Tetrahedron Lett.* **1973**, 4225-4228. (b) Cava, M. P.; Deana, A. A. *J. Am. Chem. Soc.* **1959**, *81*, 4266-4268.

(2) (a) Chapman, O. L.; McMahon, R. J.; West, P. R. *J. Am. Chem. Soc.* **1984**, *106*, 7973-7974. (b) Wentrup, C. *Reactive Molecules*; Wiley-Interscience: New York, 1984; Chapter 4.

(3) Vander Stouw, G. G. Ph.D. Dissertation, Ohio State University, Columbus, OH, 1964.

(4) Baron, W.; Jones, M., Jr.; Gaspar, P. *J. Am. Chem. Soc.* **1970**, *92*, 4739-4740.

(5) Hedaya, E.; Kent, M. *J. Am. Chem. Soc.* **1971**, *93*, 3283-3285.

(6) Shechter, H.; Vander Stouw, G. G.; Kraska, A. R. *J. Am. Chem. Soc.* **1972**, *94*, 1655-1661.

0002-7863/87/1509-0553$01.50/0